PNAS RESEARCH ARTICLE | CELL BIOLOGY

ERK and c-Myc signaling in host-derived tumor endothelial cells is essential for solid tumor growth

Zehua Zuo[a,1], Jie Liu[a,b,1], Zhihao Sun[a], Yu-Wei Cheng[a], Michael Ewing[a], Thomas H. Bugge[c], Toren Finkel[a,b], Stephen H. Leppla[d], and Shihui Liu[a,e,2]

Edited by Haian Fu, Emory University, Atlanta, GA; received July 11, 2022; accepted December 1, 2022 by Editorial Board Member R(obert) J. Collier

The limited efficacy of the current antitumor microenvironment strategies is due in part to the poor understanding of the roles and relative contributions of the various tumor stromal cells to tumor development. Here, we describe a versatile in vivo anthrax toxin protein delivery system allowing for the unambiguous genetic evaluation of individual tumor stromal elements in cancer. Our reengineered tumor-selective anthrax toxin exhibits potent antiproliferative activity by disrupting ERK signaling in sensitive cells. Since this activity requires the surface expression of the capillary morphogenesis protein-2 (CMG2) toxin receptor, genetic manipulation of CMG2 expression using our cell-type–specific CMG2 transgenic mice allows us to specifically define the role of individual tumor stromal cell types in tumor development. Here, we established mice with CMG2 only expressed in tumor endothelial cells (ECs) and determined the specific contribution of tumor stromal ECs to the toxin's antitumor activity. Our results demonstrate that disruption of ERK signaling only within tumor ECs is sufficient to halt tumor growth. We discovered that c-Myc is a downstream effector of ERK signaling and that the MEK–ERK–c-Myc central metabolic axis in tumor ECs is essential for tumor progression. As such, disruption of ERK–c-Myc signaling in host-derived tumor ECs by our tumor-selective anthrax toxins explains their high efficacy in solid tumor therapy.

anthrax lethal toxin | endothelial cells | ERK signaling | c-Myc | tumor microenvironment

Significance

We describe a versatile and highly cell-type–specific genetic platform based on the anthrax toxin protein delivery system, allowing the rigorous therapeutic assessment of individual tumor stromal cell types in tumor progression. Our approach would provide a powerful tool in understanding the tumor microenvironment, facilitating the rational design of anti-TME strategies in cancer therapy.

Cancers are a complex mixture of tumor-initiating malignant cells with oncogenic mutations combined with a variety of host-derived tumor-enabling stromal cells. The latter cell types include cancer-associated fibroblasts (CAFs), tumor endothelial cells (ECs), tumor-associated macrophages (TAMs), myeloid-derived suppressor cells, regulatory T cells (Tregs), tumor-infiltrating lymphocytes including T and B lymphocytes, and many others. In the tumor microenvironment (TME), malignant cells and the surrounding stromal cells interact dynamically through direct interactions and by indirect communications mediated by secreted molecules, such as growth factors, angiogenic factors, cytokines, chemokines, and extracellular vesicles. Tumor stromal cells are thought to regulate cancer progression through multiple mechanisms (1), such as 1) stimulation of tumor growth by TAM-induced inflammation, 2) enhancement of subsequent tumor growth and progression by enabling immune evasion, 3) induction of vessel growth (angiogenesis), and 4) eventual dissemination to secondary sites (metastasis). CAFs not only deposit extracellular matrix, an essential component of tumor tissues, but also produce matrix-remodeling enzymes, such as matrix metalloproteinases (MMPs), thereby promoting tumor invasion, metastasis, and resistance to standard-of-care therapies. In addition, CAFs promote tumor growth and invasion by secreting cytokines, exosomes, and growth factors. CAF-derived VEGF (vascular endothelial growth factor) drives angiogenesis.

Given the critical roles of tumor stromal compartment in tumor initiation and progression, strategies to therapeutically target key tumor stromal cells in the TME (such as TAMs, CAFs, T cells, and ECs) have emerged as promising approaches for cancer treatment in recent years (1, 2). However, the current anti-TME therapies in clinical evaluation usually aim to target key factors involved in intercellular communications between tumor stromal cells and cancer cells. For example, the anti-VEGF antibody bevacizumab (Avastin) was the first TME-targeted therapy approved by the FDA for treatment of metastatic colorectal cancer (3, 4). VEGF is an important angiogenic factor secreted by tumor cells and by various tumor stromal cells. However, continuous inhibition of VEGF can lead to the compensatory upregulation of other angiogenic factors and development of drug resistance (5, 6). Recently, given that engagement of the colony-stimulating factor 1 receptor (CSF1R) is important for TAMs recruitment into the TME, neutralizing antibodies and small-molecule inhibitors against CSF1R have been evaluated in patients with advanced solid tumors and metastatic diseases. However, as with anti-VEGF therapy,

Author affiliations: [a]Aging Institute of University of Pittsburgh and University of Pittsburgh Medical Center, Pittsburgh, PA 15219; [b]Division of Cardiology, Department of Medicine, University of Pittsburgh School of Medicine, Pittsburgh, PA 15219; [c]Proteases and Tissue Remodeling Section, National Institute of Dental and Craniofacial Research, NIH, Bethesda, MD 20892; [d]Microbial Pathogenesis Section, Laboratory of Parasitic Diseases, National Institute of Allergy and Infectious Diseases, NIH, Bethesda, MD 20892; and [e]Division of Infectious Diseases, Department of Medicine, University of Pittsburgh School of Medicine, Pittsburgh, PA 15219

Author contributions: S.L. designed research; Z.Z., J.L., Z.S., Y.-W.C., M.E., and S.L. performed research; T.H.B., T.F., and S.H.L. contributed new reagents/analytic tools; Z.Z., J.L., and S.L. analyzed data; and S.L. wrote the paper.

The authors declare no competing interest.

This article is a PNAS Direct Submission. H.F. is a guest editor invited by the Editorial Board.

[1]Z.Z. and J.L. contributed equally to this work.

[2]To whom correspondence may be addressed. Email: SHL176@pitt.edu.

This article contains supporting information online at https://www.pnas.org/lookup/suppl/doi:10.1073/pnas.2211927120/-/DCSupplemental.

Published December 27, 2022.

resistance to CSF1R inhibition also appears to develop (7). The limited efficacy of these and other current anti-TME strategies is due in part to the poor understanding of the roles and relative contributions of the various tumor stromal cells to tumor development. Absent this knowledge, a basis for confident selection of therapeutic targets is still missing. Therefore, robust genetic tools allowing for the therapeutic assessment of the precise role of each tumor stromal cell type in tumor development and progression are needed. Here, we describe a versatile and tractable anthrax toxin protein delivery system–based genetic platform, allowing the unambiguous evaluation of the roles of each tumor compartment in tumor progression.

Many bacterial pathogens have evolved potent protein toxins to disrupt specific pathways involved in host defense and metabolism (8–11). Fortunately, these potent, naturally occurring toxins can be structurally modified to achieve high tumor specificity (12, 13). Anthrax lethal toxin (LT), which targets the MEK–ERK pathway, represents such a toxin (14). LT is a typical A-B–type toxin consisting of two proteins: a cellular receptor-binding and delivering component termed protective antigen (PA) and an enzymatic moiety denoted as lethal factor (LF) (11, 15). To target host cells, PA binds to the cell surface receptors CMG2 (capillary morphogenesis protein-2, the major receptor) and TEM8 (tumor endothelium marker-8) (11, 15). This binding results in a proteolytic activation of PA by a cell surface furin protease, yielding the active PA oligomer (heptamer and/or octamer). The PA oligomer then binds and translocates LF into the cytosol of target cells to exert its cytotoxic effects (11, 15). The unique requirement for PA proteolytic activation on the target cell surface provides a way to reengineer PA, by modifying the protease cleavage site, so that it is activated by a tumor-associated protease rather than by furin. Therefore, we have previously successfully generated a tumor-selective PA variant termed PA-L1 that can be specifically activated by tumor-associated MMPs, thereby achieving high tumor specificity in delivering the cytotoxic effector LF or LF variant into tumor cells and tumor stromal cells (Fig. 1*A*). Since CMG2 is the major PA toxin receptor on tumor cells and tumor stromal cells, to avoid damaging normal tissues such as the kidneys and brain that express the TEM8 receptor (16, 17), we also generated a CMG2-specific version of PA-L1, namely PA-L1-I656Q (18, 19), which has a similar antitumor activity as PA-L1 when combined with LF.

Since the antitumor activity of PA-L1-I656Q/LF absolutely requires the presence of CMG2 receptor on target cells (19) (Fig. 1*A*), we reasoned that, by genetically manipulating the expression pattern of CMG2 on cancer cells and each tumor stromal cell type, we can selectively target the toxin to specific cell types and thereby unambiguously determine the specific contribution of each of these cell types to the toxin's antitumor activity. Cell-type–specific expression of CMG2 can be conveniently achieved by using our previously generated cell-type–specific CMG2 gain-of-function and loss-of-function mice (12, 16, 20, 21). We hypothesized that by examining the responses of implanted tumors lacking the CMG2 receptor to our engineered tumor-selective MEK-inactivating toxin, we could define the role of each tumor stromal cell type, such as tumor ECs (22), TAMs (23), CAFs (24, 25), B cells (26), and Tregs (27, 28), in tumor progression. Using this tumor–host genetic platform, we found that MEK–ERK signaling in tumor ECs plays an essential role in tumor progression. We discovered that c-Myc, a master transcription factor controlling central metabolism, is an effector protein downstream of MEK–ERK and that disruption of the MEK–ERK–c-Myc bioenergetic axis in tumor ECs may be an efficient strategy to inhibit tumor growth.

Results

A Unique Genetic Platform for Assessing Tumor Stromal Compartment. We have developed a series of highly tumor-selective anthrax LTs with potent antitumor activity against a wide range of tumors (13, 29–35). One of these reengineered toxins, termed PA-L1-I656Q/LF, relies strictly on the toxin receptor CMG2 and tumor-associated MMPs to gain entry into target cells (Fig. 1*A*). PA-L1-I656Q/LF exhibited potent *in vivo* antitumor activity toward human C32 melanoma cells, which contain a $BRAF^{V600E}$ mutation, thereby relying on MEK–ERK signaling for survival (*SI Appendix*, Fig. S1*A*). Interestingly, this engineered toxin also demonstrated efficacy to tumors formed by cancer cells lacking the CMG2 receptor. We found that mouse syngeneic tumors formed from CMG2-deficient Lewis lung carcinoma (LLC(CMG2KO)) cells and mouse B16-F10 melanoma (B16(CMG2-KO)) cells were also responsive to PA-L1-I656Q/LF treatment (*SI Appendix*, Fig. S1 *B* and *C*), attesting to the critical role of the tumor stromal compartment in tumor progression. Therefore, we reasoned that manipulation of CMG2 expression in specific cell types of the TME, combined with toxin administration, could explicitly delineate the roles in tumor progression of a given tumor stromal cell type.

Cell-type–specific expression of CMG2 can be conveniently achieved by using our previously generated CMG2 transgenic mice, in which the CMG2 transgene is under the control of the CAG promoter but its expression is blocked by a LoxP-Stop-LoxP (LSL) cassette ($CMG2^{LSL}$) (Fig. 1*B*) (16, 20, 21). Thus, these transgenic mice do not express the CMG2 transgene until they are mated with cell-type–specific Cre transgenic mice so that the LSL cassette is excised (Fig. 1*B*). This system allows a cell-type–specific restoration of CMG2 expression within the context of the whole-body $CMG2^{-/-}$ mice that we generated previously (16). For example, the host-derived endothelial cell–specific CMG2-expressing mice ($CMG2^{LSL}$;*Cdh5-Cre*;$CMG2^{-/-}$, hereafter referred to $CMG2^{EC}$) were obtained by breeding $CMG2^{LSL}$ mice with *Cdh5-Cre* (endothelial cell–specific Cre transgenic) mice to activate the CMG2 transgene expression only in ECs within the context of $CMG2^{-/-}$ mice (Fig. 1 *C*–*E*). Similarly, other cell-type–specific CMG2-expressing mice could also be readily generated by breeding with the respective cell-type–specific Cre transgenic mice (21). We postulated that when tumors lacking CMG2 are established in these mice and are subsequently treated with the engineered toxin LF/PA-L1-I656Q, these tumor–host toxin tractable genetic systems would allow us to determine the role of specific tumor stromal cell types in tumor development. Because the toxin exerts its cytotoxic action through disruption of ERK signaling, this approach would also allow us to define the role of ERK signaling in specific tumor stromal cell types in tumor progression. Host-derived tumor stromal ECs are an important prototype of stromal cells in the TME. Therefore, in this study, as an example of using our unique tumor–host toxin genetic platform, we sought to determine the specific role of ERK signaling in tumor stromal ECs in tumor development (Fig. 1*F*).

ERK Signaling in Stromal ECs Is Essential for Tumor Development. We first verified the endothelial cell–specific expression of CMG2 in $CMG2^{EC}$ mice. We isolated primary ECs by sorting ICAM2-positive ECs from the lungs of $CMG2^{EC}$ mice and their littermate control mice. The identity of the isolated ECs (ICAM2 positive) was confirmed by positive staining with CD31, another endothelial cell marker (Fig. 1*C*). As expected, while the nonendothelial cell fraction (ICAM2 negative) was resistant to PA-I656Q in the presence of effector FP59 (PA-I656Q/FP59),

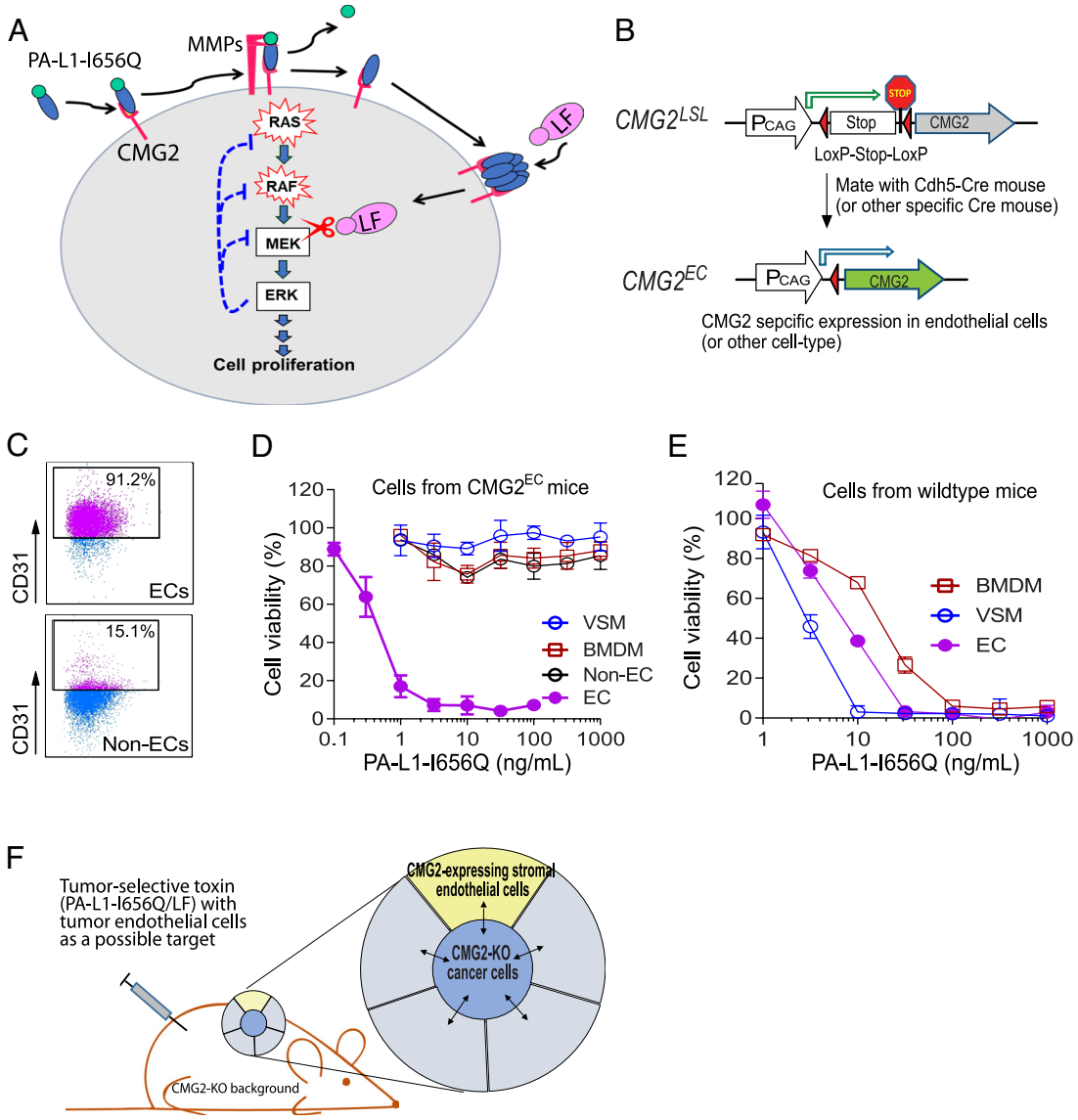

Fig. 1. Anthrax toxin receptor CMG2-based tumor–host genetic platform for assessing tumor ECs. (*A*) Anthrax toxin protein delivery system as a unique platform for cancer therapy with high specificity. Tumor specificity of PA-L1-I656Q is achieved by engineering the delivering vehicle PA to bind to the CMG2 receptor and rely on tumor-associated proteases (MMPs) for activation. Thus, LF (or LF fusions) can be selectively delivered into tumor cells and tumor stromal cells to inactivate MEK1/2, disrupting the ERK signaling. (*B*) Generation of endothelial cell–specific CMG2 receptor–expressing mice. Breeding of *CMG2*^{LSL} and *Cdh5-cre* mice allowed specific removal of the LoxP-Stop-LoxP cassette and subsequent activation of the CMG2 transgene only in ECs. Subsequent breeding with whole-body *CMG2*$^{-/-}$ mice eliminated expression of the endogenous CMG2 gene, resulting in a mouse where only ECs express CMG2 (*CMG2*^{EC}). Similarly, we can generate other tumor stromal cell-type–specific CMG2-expressing mice by using the corresponding cell-type–specific Cre transgenic mouse. (*C*) The identity of primary ECs isolated from *CMG2*^{EC} mice was verified by the second endothelial marker CD31-positive staining. Flow cytometry analyses of ECs (ICAM2 positive) and nonECs (ICAM2 negative) bound with a CD31 antibody. (*D* and *E*) Primary cells from *CMG2*^{EC} (*D*) and wild-type control (*E*) mice were treated with various concentrations of PA-L1-I656Q in the presence of FP59 (100 ng/mL) for 48 h, followed by an MTT assay evaluating cell viability. Of note, only ECs from *CMG2*^{EC} mice were sensitive to PA-L1/FP59, whereas non-ECs (ICAM2 negative), VSMs, and BMDMs were resistant to the toxin. (*F*) A tumor–host model with tumor ECs as an only possible target. Tumors contain tumor-initiating malignant cells and a variety of tumor stromal cells, which cooperate to promote tumor growth. In this example, only tumor ECs express the toxin receptor CMG2, thereby allowing unambiguous assessment of the role of this tumor stromal cell type in the targeted therapy using the engineered toxin. The same approach could be adapted to evaluate the roles of other tumor stromal cell types in tumor development.

isolated ECs were exquisitely sensitive to the toxin (Fig. 1*D*). FP59 is a fusion protein of LF amino acids 1–254 and the catalytic domain of *Pseudomonas aeruginosa* exotoxin A that kills cells by ADP-ribosylation of eEF2 after delivery to the cytosol by PA (36). Furthermore, we also isolated the primary bone marrow–derived macrophages (BMDMs) and the vascular smooth muscle cells (VSMs) from *CMG2*^{EC} mice and their littermate wild-type control mice. While BMDMs and VSMs derived from *CMG2*^{EC} mice were resistant to PA-I656Q/FP59 (Fig. 1*D*), the corresponding cells derived from wild-type littermate mice were, as expected, sensitive to the toxin (Fig. 1*E*). Therefore, we assumed that when growing syngeneic CMG2-deficient tumors in *CMG2*^{EC} mice, only the ECs in the tumor stromal compartment would express the toxin receptor CMG2, thereby being the only cell type susceptible to our engineered tumor-selective anthrax LT (Fig. 1*F*).

B16-F10 melanoma cells have been widely used to form syngeneic tumors in mice. To grow tumors that have the host-derived tumor stromal compartment as an only possible target, we generated CMG2-deficient B16-F10 cells using CRISPR/Cas9 genome editing. Aligning well with the essential role of CMG2 as the toxin receptor, the B16(CMG2-KO) cells were completely resistant to PA-I656Q/FP59, whereas the parental wild-type cells were highly sensitive to the toxin (Fig. 2*A*). Furthermore, LF could be delivered into the cytosol of the wild-type cells by PA-I656Q, leading

to MEK1/2 cleavage and the associated disruption of the ERK signaling (Fig. 2*B*). As expected, PA-I656Q/LF had no effect on B16(CMG2-KO) cells (Fig. 2*B*). When injected into C57BL/6J mice, B16(CMG2-KO) cells formed highly angiogenic tumors (~50 to 80 mm^3) within 10 d after injection into C57BL/6J mice (*SI Appendix*, Fig. S2*A*).

We then inoculated B16(CMG2-KO) cells into the $CMG2^{EC}$ mice and the whole-body $CMG2^{-/-}$ mice. B16(CMG2-KO) cells retained the ability to form rapidly growing tumors in both $CMG2^{EC}$ and $CMG2^{-/-}$ mice, demonstrating that the presence of CMG2 on tumor cells, as well as the host-derived tumor stromal cells, is not required for B16-F10 tumor development (Fig. 2 *C* and *D*). Next, B16(CMG2-KO) tumor-bearing mice were randomized and treated with either PBS or PA-L1-I656Q/LF (Fig. 2 *C* and *D*). In the tumor–host setting of $CMG2^{-/-}$ mice, both malignant cells (B16(CMG2-KO)) and the host-derived tumor stromal compartment are not targets of the tumor-selective toxin due to the absence of the CMG2 receptor. As expected, the B16(CMG2-KO) tumors grown in $CMG2^{-/-}$ mice were completely resistant to PA-L1-I656Q/LF (Fig. 2*C*). In contrast, the same tumors grown in $CMG2^{EC}$ mice were highly susceptible to the same toxin treatment (Fig. 2*D* and *SI Appendix*, Figs. S2*B* and S3). Since only the host-derived tumor ECs express CMG2, this result demonstrates that tumor ECs are essential for tumor progression and that endothelial ERK signaling is required for the tumor-promoting functions of this essential tumor stromal cell type.

With the above results demonstrating that targeting tumor ECs is sufficient to inhibit tumor growth, we next sought to assess

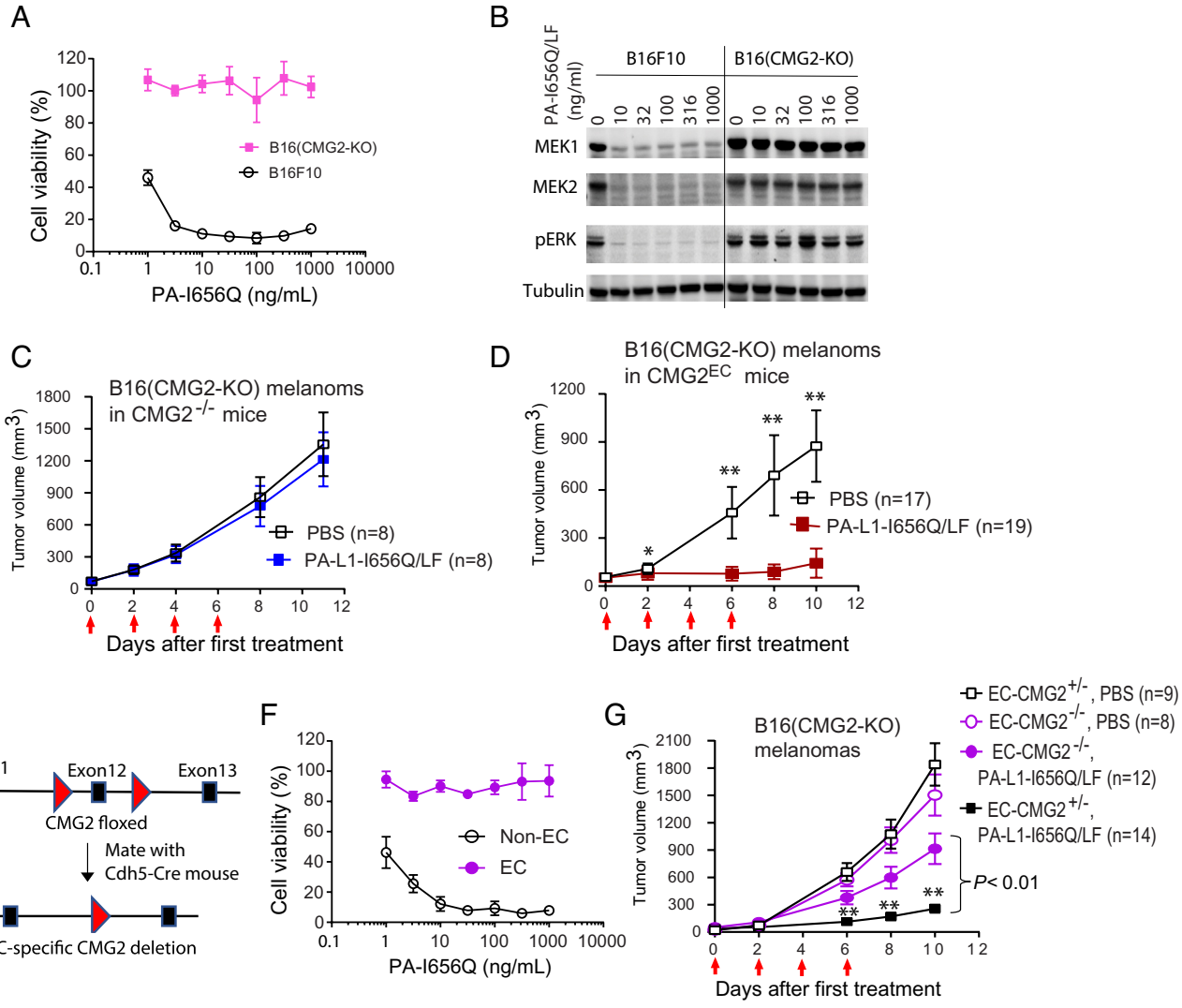

Fig. 2. Disruption of the MEK–ERK signaling in tumor ECs is sufficient to inhibit tumor growth. (*A*) B16-F10 (CMG2-KO) cells are resistant to the CMG-specific PA-L1-I656Q/FP59. B16-F10 cells (WT) and B16-F10 (CMG2-KO) cells were incubated with various concentrations of PA-L1-I656Q in the presence of 100 ng/mL FP59 for 48 h, followed by an MTT assay for assessing cell viability. (*B*) MEK cleavage and ERK phosphorylation do not occur in B16(CMG2-KO) cells treated with PA-L1-I656Q/LF. B16-F10 cells (WT) and B16-F10 (CMG2-KO) cells were incubated with various concentrations of PA-L1-I656Q/LF for 3 h. Then, cell lysates were prepared and analyzed by western blotting using anti-MEK1, anti-MEK2, and anti-phospho-ERK antibodies. Of note, while LF could be efficiently delivered into WT B16-F10 cells, resulting in MEK cleavage and disruption of the ERK signaling, this could not occur in B16-F10 (CMG2-KO) cells. (*C*) B16(CMG2-KO) melanomas grown in $CMG2^{-/-}$ mice were completely resistant to the PA-L1-I656Q/LF [4 × (30 μg/10 μg)] treatments. Toxin treatments indicated by red arrows. Tumors, mean ± SE. No significant difference. (*D*) B16(CMG2-KO) melanomas grown in $CMG2^{EC}$ (endothelial cell–specific CMG2-expressing) mice are sensitive to the PA-L1-I656Q/LF [4 × (30 μg/10 μg)] treatments. Tumors (mean ± SE) and body weight (mean ± SD) (*SI Appendix*, Fig. S3) were monitored. $*P < 0.05$ and $**P < 0.01$. (*E*) Generation of endothelial cell–specific CMG2-null ($EC\text{-}CMG2^{-/-}$) mice. (*F*) Primary ECs and ICAM2-negative nonECs from $EC\text{-}CMG2^{-/-}$ mice were treated with various concentrations of PA-I656Q in the presence of FP59 (100 ng/mL) for 48 h, followed by an MTT assay evaluating cell viability. (*G*) B16(CMG2-KO) melanoma-bearing $EC\text{-}CMG2^{-/-}$ mice and their littermate control ($EC\text{-}CMG2^{+/-}$) mice were treated with PA-L1-I656Q/LF (30 μg/10 μg) as indicated by arrows. Of note, B16(CMG2-KO) melanomas are much less sensitive to the toxin when grown in $EC\text{-}CMG2^{-/-}$ mice. EC-$CMG2^{+/-}$ (PA-L1-I656Q/LF) vs. other groups, $P < 0.01$, and no statistically significant difference among other groups. Tumors (mean ± SE) and body weight (mean ± SD) (*SI Appendix*, Fig. S3) were monitored. $**P < 0.01$.

whether ERK signaling in this tumor stromal cell type is necessary for tumor progression. To address this, we generated endothelial cell–specific CMG2 knockout mice (hereafter referred to *EC-CMG2*$^{-/-}$ mice) by breeding the CMG2-floxed mice [we generated previously (16)] with *Cdh5-Cre* transgenic mice (Fig. 2*E*). As expected, the primary ECs from *EC-CMG2*$^{-/-}$ mice were completely resistant to PA-I656Q/FP59, whereas the non-ECs from the same mice were highly sensitive to the toxin (Fig. 2*F*). We then inoculated B16(CMG2-KO) cells in *EC-CMG2*$^{-/-}$ mice and their littermate *EC-CMG2*$^{+/-}$ mice. The resulting B16(CMG2-KO) tumor-bearing mice were treated with PA-L1-I656Q/LF. In the tumor–host setting of *EC-CMG2*$^{-/-}$ mice where malignant cells and stromal ECs were not possible targets, the B16(CMG2-KO) tumors exhibited significantly reduced susceptibility to our engineered toxin compared with the tumors grown in *EC-CMG2*$^{+/-}$ mice (Fig. 2*G* and *SI Appendix*, Fig. S3), indicating that an intact MEK–ERK signaling in tumor ECs is critical for tumor development. Interestingly, these tumors were still, although to a lesser extent, responsive to PA-L1-I656Q/LF treatments (Fig. 2*G*). This suggests that other stromal cells likely contribute to the overall antitumor activity of the toxin.

Profound Inhibitory Effects of the Engineered Toxin on Metabolism of Tumor ECs. To further investigate how disruption of ERK signaling affects tumor endothelial cell function, we isolated primary ECs from B16-F10 tumors through ICAM2-positive sorting and treated the cells with PA-L1/LF (Fig. 3 *A*–*C*). Surprisingly, even after 72-h incubation, the toxin did not directly kill ECs as judged by microscopic observation, trypan blue staining, or annexin V plus propidium iodide staining (Fig. 3*B* and *SI Appendix*, Fig. S4). In contrast, when FP59 was used as the effector protein, the majority of ECs were killed within 24 h (Fig. 3*B*). Instead, however, PA-L1/LF displayed potent inhibitory activity on endothelial cell proliferation (Fig. 3*C*). In addition, we found that within 24 h, the phenol red in the culture medium (as a pH indicator) consistently turned a bright pink color (> pH.8.2) when the cells were incubated with PA-L1/LF, suggesting that cellular glycolytic metabolism and secretion of lactic acid might be affected by the toxin.

Based on these observations and the fact that cellular metabolism is crucial for all cellular processes (37, 38), we used the Seahorse technology to determine whether PA-L1/LF affects the bioenergetics of tumor ECs. Thus, we measured the extracellular acidification rates (ECARs) and oxygen consumption rates (OCRs) of tumor ECs under basal conditions and also following addition of the mitochondrial inhibitors oligomycin (ATP synthase inhibitor), FCCP (mitochondrial oxidative phosphorylation uncoupler), and antimycin A (complex III inhibitor) (Fig. 3 *D* and *E*). ECAR reflects cytosolic glycolytic activity, whereas OCR reflects the activity of mitochondrial oxidative phosphorylation. Interestingly, PA-L1/LF significantly inhibited endothelial cell glycolytic activity and oxygen consumption under basal conditions and when mitochondria were inhibited (Fig. 3 *D* and *E*). Interestingly, these potent metabolic inhibitory effects could be closely recapitulated by the MEK inhibitor Trametinib (Fig. 3 *D* and *E*). The compensatory upregulation of glycolytic activity in response to diminished energy production during mitochondrial inhibition (by oligomycin and FCCP) was also compromised by the toxin and Trametinib (Fig. 3 *D* and *E*). Furthermore, cellular ATP levels of tumor ECs were also markedly decreased by the toxin (Fig. 3*F*). These results demonstrate that disruption of ERK signaling by the toxin profoundly affects tumor endothelial cell metabolism, altering both glycolysis and mitochondrial oxidative phosphorylation.

Disruption of ERK Signaling by the Toxin Suppresses c-Myc Expression. To explore the mechanisms underlying the toxin's effects on metabolism of ECs, we surveyed the expression levels of a panel of genes key to central metabolism by quantitative real-time PCR analyses (Fig. 3*G*). Surprisingly, many genes that regulate glucose uptake (*Glut-1*), glycolysis (*G6PD*, *Hk1*, *Gapdh*, *Ldha*, and *Ldhb*), tricarboxylic acid (TCA) cycle metabolism (*Pdha1*, *Cs*, *Idh2*, and *Fh*), glutamine usage (*Slc1a5*, *Glud1*, and *Gls1*), and lipid synthesis (*Acly*, *Hmgcr*, *Fasn*, *Dgat1*, and *Elovl6*) were significantly down-regulated after PA-L1/LF treatment. The transcription factors c-Myc and HIF1α are master regulators of central metabolism (39, 40). Remarkably, *c-Myc* was the most affected early response gene with an expression level reduced to 17% and 10% of the untreated controls at 4 h and 24 h, respectively. In addition, the LF-mediated MEK1/2 cleavage and ERK signaling disruption could be efficiently detected in a dose-dependent manner, accompanied by downregulation of c-Myc at the protein level in the toxin-treated ECs (Fig. 3*H* and *SI Appendix*, Fig. S5 *A* and *B*). This potent inhibitory effect could be completely recapitulated by the MEK inhibitor Trametinib (Fig. 3*H*). These findings may also apply to many other cells because c-Myc expression in HT29 (human colorectal carcinoma), A2058 (human melanoma), RKO (human colorectal carcinoma), MiaPaCa-2 (human pancreatic carcinoma), and B16-F10 cells was also down-regulated by PA-L1/LF (*SI Appendix*, Fig. S5*C*). These results demonstrate that c-Myc is an important effector of the ERK signaling in tumor ECs and potentially other cell types. Since glucose and glutamine are the two major carbon sources for catabolic metabolism (ATP production) and anabolic metabolism (macromolecule syntheses), and lipid synthesis provides essential plasma membrane building blocks for cell proliferation; the profound effects of the toxin on tumor growth may be, at least in part, attributed to the disruption of the MEK–ERK–c-Myc bioenergetic axis in tumor ECs.

c-Myc Transgene Rescues Metabolic Stress Caused by the Toxin. To further explore the essential role of c-Myc in endothelial metabolism, we attempted to generate endothelial cell–specific c-Myc-expressing mice by breeding the LoxP-Stop-LoxP c-Myc transgenic mice (*c-Myc*^{LSL}, Jackson Laboratory #020458) with *Cdh5-Cre* mice (*SI Appendix*, Fig. S6*A*), allowing the specific expression of the c-Myc transgene only in ECs (*c-Myc*^{LSL};*Cdh5-Cre*, referred to *c-Myc*^{EC} mice hereafter). Unexpectedly, *c-Myc*^{EC} mice exhibited underdeveloped phenotypes with a significant decrease in body weight after birth (*SI Appendix*, Fig. S6*B*). Unfortunately, the *c-Myc*^{EC} mice also showed much earlier onset of mortality, with 50% and 100% of the mice dying by 10 and 18 wk of age, respectively (*SI Appendix*, Fig. S6*C*). These results demonstrate that constant expression of c-Myc in ECs has deleterious effects on normal growth and development. Although the poor health conditions of the *c-Myc*^{EC} mice prevented us from further assessing the in vivo role of c-Myc in tumor ECs in tumor progression, we were able to isolate primary ECs from the *c-Myc*^{EC} and their littermate control mice (*Cdh5-Cre* negative, referred to WT here). Although ECs are quiescent in vivo, they rapidly turn into quickly proliferating ECs when cultured in growth medium supplemented with endothelial cell growth supplement (Sigma, E2759) containing VEGF, FGF2, and other growth factors (mimicking the in vivo "angiogenic switch on" conditions), reasonably modeling tumor ECs.

Since the c-Myc transgene is under the control of the ubiquitous CAG promoter rather than *c-Myc*'s endogenous promoter, the expression of the c-Myc transgene in *c-Myc*^{EC} ECs was only partially affected by PA-L1/LF and Trametinib (Fig. 4*A*). To examine

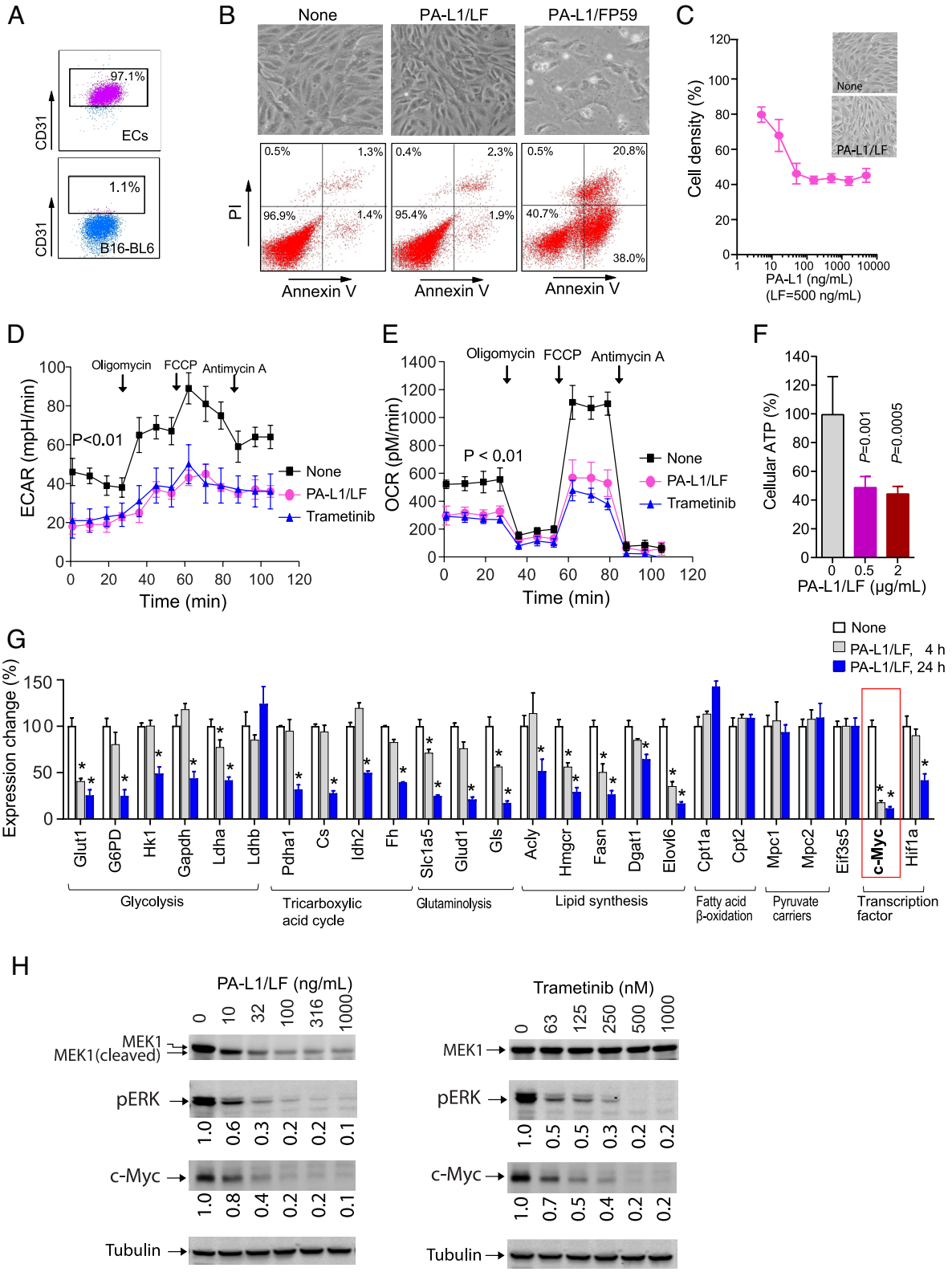

Fig. 3. Effects of the engineered LT on metabolism of tumor ECs. (*A*) Flow cytometry analyses of tumor ECs (ICAM2-positive) and B16-F10 cells bound with a CD31 antibody. (*B*) Tumor ECs were incubated with or without PA-L1/LF (1 μg/mL each) for 72 h or with PA-L1/FP59 (0.1 μg/mL each) for 24 h. *Upper*: microscopic views of the cells after the treatments. Note, the cells were still viable 72 h after PA-L1/LF treatments. In contrast, the cells treated with PA-L1/FP59 for 24 h were mostly dead, with only a small number of swollen damaged cells remaining attached. *Lower*: flow cytometry analyses of the cells stained with propidium iodine (PI) and annexin V. Note, 95% of the cells treated with PA-L1/LF were still alive (vs. 97% alive for the untreated cells). (*C*) Tumor ECs cultured in 96-well plates were incubated with various concentrations of PA-L1 in the presence of LF (500 ng/mL) for 72 h; MTT assays were followed to evaluate cell numbers relative to the nontoxin-treated wells. Data are shown as mean ± SD. *Inset*, microscopic views of tumor ECs treated with or without PA-L1/LF (1 μg/mL each) for 72 h. (*D*) Tumor ECs were treated with or without PA-L1/LF (1 μg/mL each) or Trametinib (0.2 μM) for 24 h; then, the ECARs were measured using the Seahorse XF24 analyzer under basal conditions and following sequential addition of ATP synthase inhibitor oligomycin (0.5 μg/mL), uncoupler FCCP (1 μM), and complex III inhibitor antimycin A. The ECAR readings were normalized to amounts of cells having 50 μg total protein, mean ± SD. Paired Student's *t* test, $P < 0.0001$. (*E*) The OCRs of tumor ECs treated under the same conditions as in *D* were measured using the Seahorse XF24 analyzer. The OCR readings were normalized to 50 μg of

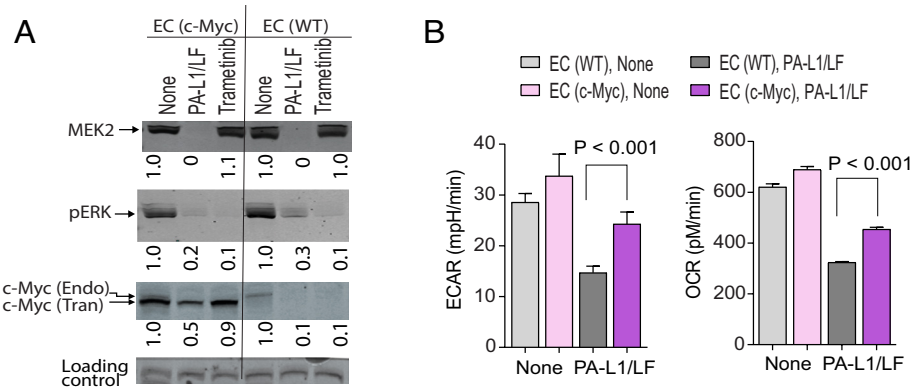

Fig. 4. Expression of the c-Myc transgene in primary ECs partially rescued the metabolic stress caused by the engineered toxin. (*A*) Primary ECs isolated from c-MycEC or their littermate control (WT) mice were treated with PA-L1/LF (1 μg/mL) or Trametinib (0.2 μM) for 3 h. Then, cell lysates were prepared and analyzed by western blotting. Both PA-L1/LF and Trametinib could efficiently disrupt the ERK signaling in both WT and c-MycEC ECs. However, c-Myc was only partially affected by PA-L1/LF and Trametinib in c-MycEC ECs. (*B*) The metabolic crisis caused by PA-L1/LF was partially rescued in ECs from the c-MycEC mice. ECs were treated with or without PA-L1/LF (1 μg/mL each) for 24 h; then, the ECARs (*Left*) and OCRs (*Right*) were analyzed as described in Fig. 3. The ECAR and OCR readings were normalized to 50 μg of total protein, mean ± SD. EC (c-Myc) (PA-L1/LF) vs. EC (WT) (PA-L1/LF), $P < 0.01$, paired Student's *t* test.

whether this "toxin-resistant" c-Myc could rescue the metabolic crisis caused by PA-L1/LF, we measured the ECARs and OCRs of the ECs under basal condition. We found that the toxin-induced metabolic inhibition could be significantly mitigated by the expression of the toxin-resistant c-Myc (Fig. 4*B*). These results further strengthen the notion that the toxin's inhibitory effects occur through the disruption of the MEK–ERK–c-Myc bioenergetic axis in tumor ECs, thereby modulating the central metabolism of host-derived ECs.

Discussion

Here, we describe a versatile and highly cell-type–specific genetic platform based on anthrax toxin and its cellular receptor, allowing the rigorous genetic assessment of individual tumor stromal cell types in tumor progression. We provide an example of this unique system to reveal the role of tumor ECs in tumor development. We demonstrate that tumor ECs are a viable target for cancer therapy and that disruption of the MEK–ERK–c-Myc biogenetic axis in this tumor stromal cell type is sufficient to halt tumor growth.

Tumor ECs Are a Viable Target for Cancer Therapy. In solid tumors, the "angiogenic switch" converts host-derived quiescent ECs into rapidly proliferating tumor ECs responsible for the support and growth of rapidly growing (22, 41) tumors. Therefore, activated tumor ECs will likely exhibit a high demand for energy production and macromolecular synthesis (such as amino acids, lipids, and nucleotides) to fuel replication. We discovered that our tumor-selective toxin has potent inhibitory activities on both cytosolic glycolysis and mitochondrial oxidative phosphorylation, the central metabolic pathways responsible for both bioenergetic production and biosynthesis of macromolecules needed for cell replication. Mechanistically, the inhibition of cellular central metabolism of tumor ECs occurs through the rapid inhibition of c-Myc at both the mRNA and protein levels. c-Myc is a master transcription factor having an established role as a transcriptional amplifier of many key genes involved in cellular metabolic activities. Interestingly, we found that disruption of ERK signaling by our toxin resulted in 2- to 8-fold decrease in the expression of the affected metabolic genes. This agrees well with the fact that c-Myc amplifies the expression of genes that are basally expressed, usually resulting in a 2- to 12-fold increase in their expression (39, 42).

c-Myc as a Downstream Effector of the ERK Signaling. c-Myc is a known oncogene, and deregulation of c-Myc occurs in 50% of all human cancers (43). However, c-Myc is deemed to be a poor therapeutic target because it lacks a druggable interface and because its activity is essential for maintaining normal tissue homeostasis. ERK has an established role in regulating c-Myc at the posttranscriptional level by directly phosphorylating Ser62, which in turn increases c-Myc transcriptional activity (44, 45). Therefore, our findings offer an approach for targeting c-Myc transcription in tumor ECs and potentially other tumor stromal cells and cancer cells through disruption of ERK signaling. Since our engineered toxins exhibit high tumor specificity, these toxins might have advantages as therapies for c-Myc–dependent tumors via indirectly targeting ERK–c-Myc signaling.

Tumor ECs vs. Normal ECs. In sharp contrast to tumor ECs, which are highly proliferative, normal ECs are mostly quiescent in vivo (estimates suggest replication occurs every 1,000 d) (46). This suggests that quiescent ECs have very limited biosynthetic requirements and thus are largely insensitive to the engineered toxin. This assumption is consistent with our previous finding that normal ECs are not a major target of anthrax LT (12) and that $CMG2^{EC}$ (having toxin receptor only expressed in ECs) mice are highly resistant to wild-type (furin-activated version) anthrax LT. This is in sharp contrast to our observation that B16(CMG2-KO) tumors grown in these mice are highly sensitive to the toxin. This argues that the engineered toxin is highly selective for tumor versus normal ECs not only because of the abundance of tumor-

total protein, mean ± SD. Paired Student's *t* test, $P = 0.0019$. (*F*) The relative cellular ATP levels of tumor ECs treated with PA-L1/LF (0.5 μg/mL or 2 μg/mL each) for 24 h vs. untreated cells. Data are shown as mean ± SD. (*G*) Real-time PCR analyses of selected key genes in central metabolism of tumor ECs treated with or without PA-L1/LF (1 μg/mL each) for 4 h or 24 h. Eukaryotic translation initiation factor *Eif3s5* was used as an internal normalization control. The full names of the genes can be found in *SI Appendix*, Table S1. Note, *Cpt1a, Cpt2, Mpc1, Mpc2,* and *Eif3s5* are among the genes not affected by the toxin. Student's *t* test: $*P < 0.01$. (*H*) Downregulation of c-Myc at the protein level following the ERK signaling disruption. Tumor ECs were incubated with various concentrations of PA-L1/LF or Trametinib for 3 h. Then, cell lysates were prepared and analyzed by western blotting using antibodies as indicated. The relative protein band densities estimated using ImageJ were shown below each lane.

associated proteases (MMPs) in the TME but also due to intrinsic difference in cellular metabolism.

Although normal ECs are largely quiescent in vivo, they can rapidly switch to a highly proliferative state when cultured in growth medium, commonly supplemented with endothelial cell growth supplements containing VEGF, FGF2, and related factors, mimicking the in vivo angiogenic switch conditions. Therefore, primary ECs isolated from tumors and normal tissues, such as the lungs, are expected to be similar in their proliferation and their metabolic demands. In fact, we observed that primary ECs isolated from the wild-type lungs and from tumors are both sensitive to the inhibitory effects of the engineered toxin and to Trametinib.

Tumor-Selective Toxin vs. Small-Molecule MEK Inhibitor. Cancer driver mutations in the RAS–RAF–MEK–ERK pathway occur in 46% of all human cancers. This has inspired the successful development of many small-molecule inhibitors of MEK (such as Trametinib). Although these FDA-approved agents have benefited some patients with metastatic melanomas containing BRAF mutations, their therapeutic index is low. These MEK inhibitors are designed to target ERK signaling in tumors with BRAF mutations. Our results suggest that disruption of the ERK signaling in tumor ECs is likely to also contribute to the antitumor mechanisms of these agents. ERK pathway inhibition by small-molecule MEK inhibitors can activate a negative feedback circuit often leading to ERK pathway reactivation. This pathway reactivation is a common mechanism through which cancer cells develop resistance to these small-molecule MEK inhibitors. In this context, since our toxin can irreversibly (proteolytically) inactivate MEK, RAS–RAF–MEK–ERK pathway reactivation is unlikely to occur in cancers treated with our engineered toxin.

Versatility of Our Genetic Platform for Assessing Tumor Stromal Compartment. In addition to tumor ECs, our tumor–host genetic platform can be readily adapted to investigate the roles of other key tumor stromal cell types in tumor development. Generation of mice with the CMG2 receptor expressed only in distinct tumor stromal cell types, such as TAMs, CAFs, and Tregs (27, 28), can be achieved by breeding $CMG2^{LSL}$ mice with the corresponding cell-type–specific Cre-expressing mice. For example, Csf1r-Cre (stock no. 029206), aSMA-Cre (stock no. 029206), and Foxp3-Cre (stock no. 016959) transgenic mice available from Jackson Laboratory can be used to generate tumor–host mice with CMG2 expressed only in TAMs, CAFs, and Tregs (27, 28), respectively. When coupled with toxin targeting, these tumor models should allow one to explicitly define the role of these tumor stromal cell types in tumor development.

In addition to its potential in offering cell-type specificity, the anthrax toxin protein delivery system may also be used to deliver a variety of payload effector proteins into target cells by simply fusing the "passenger" polypeptides with LFn, the N-terminal domain of LF (the PA-binding domain consisting of aa 1 to 254). The fusion proteins can thus be delivered to the cytosol of target cells in a PA-dependent process. As such, LFn fusions to other bacterial toxin enzymatic domains, such as the ADP-ribosylation domain of *Pseudomonas* exotoxin A (FP59) (36, 47), the A subunit of diphtheria toxin (48), and the A subunit of Shiga toxin (49), have been constructed and were used to kill cells possessing anthrax PA receptors. Recently, LFn fusions with Cre recombinase and DUF5 toxin have been created. LFn–Cre was used to image anthrax toxin–targeted cells in the mTmG reporter mice (17). DUF5, the multifunctional-autoprocessing repeats-in-toxin (MARTX) toxin effector domain from *Vibrio vulnificus*, was identified to be a specific endopeptidase that cleaves within RAS proteins (between Y32 and D33), thereby inactivating both wild-type and mutant RAS proteins expressed in malignancies (9). Therefore, while LFn–DUF5 could be used as a potent payload of our tumor-selective engineered toxins for targeting cancers with oncogenic RAS mutations, it could also be used in combination with our toxin delivery system to determine the roles of RAS signaling in various tumor compartments.

Conclusions

We have developed a versatile and tractable genetic platform for assessing the role of individual and distinct tumor stromal components in tumor progression. As a first example, we demonstrate that tumor ECs are a viable target for cancer therapy. Our results reveal that c-Myc is a downstream effector of ERK signaling and that the MEK–ERK–c-Myc central metabolic axis in tumor ECs is essential for tumor progression. Therefore, disruption of the MEK–ERK–c-Myc central metabolic axis within tumor ECs is sufficient to halt tumor growth.

Materials and Methods

Proteins and Reagents. Recombinant PA variants and LF proteins were purified from supernatants of BH480, an avirulent, sporulation-defective, protease-deficient *B. anthracis* strain, as described previously (50, 51). PA-L1 is a MMP-activated PA variant, in which the furin cleavage sequence RKKR (residues 164 to 167) is replaced with a MMP substrate sequence GPLGMLSQ (34). PA-L1-I656Q is a PA-L1 variant with I656Q mutation in PA domain 4. PA-L1-I656Q cannot bind to the TEM8 receptor but retains binding affinity for the CMG2 receptor. FP59 is a fusion protein of LF amino acids 1 to 254 and the catalytic domain of *P. aeruginosa* exotoxin A that kills cells by ADP-ribosylation of eEF2 after delivery to the cytosol by PA (36). The LF and FP59 used here contain the native amino-terminal sequence AGG (50). MTT (3-[4,5-dimethylthiazol-2-yl]-2,5-diphenyltetrazolium bromide) was from Sigma.

Cells and Cytotoxicity Assay. All cultured cells were grown at 37 °C in a 5% CO_2 atmosphere. LLC cells (52) were originally from Judah Folkman (Harvard Medical School). Murine melanoma B16-F10 cells, human lung carcinoma A549 cells, colorectal carcinoma HT-29, Colo205 cells, and melanoma A2508 cells were from ATCC. Human cancer cells were authenticated by sequencing the featured oncogenic mutations in these cells. All tumor cells were cultured in DMEM supplemented with 10% fetal bovine serum. Mouse primary ECs and tumor ECs from B16-F10 melanomas were isolated following the protocol for endothelial cell isolation (53). Briefly, mouse lungs and B16-F10 tumors were digested with type I collagenase and plated on gelatin and collagen-coated flasks. The cells were then subjected to sequential negative sorting by magnetic beads coated with a sheep anti-rat antibody using a Fc blocker (rat anti-mouse CD16/CD32, catalog no. 553142, BD Pharmingen) to remove macrophages and positive sorting by magnetic beads using an anti-intermolecular adhesion molecule 2 (ICAM2 or CD102) antibody (catalog no. 553326, BD Pharmingen) to isolate ECs. NonECs from the lungs (defined as the ICAM2-negative cells) were also isolated. ECs were cultured in DMEM supplemented with 20% fetal bovine serum, endothelial cell growth supplement (30 mg in 500 mL DMEM) (E2759, Sigma) from bovine neural tissue (containing both acidic and basic fibroblast growth factors), and heparin (50 mg in 500 mL DMEM) (H3149-100 KU, Sigma).

To generate LLC(CMG2-KO) and B16(CMG2-KO) cells by CRISPR gene editing, we cloned the mouse CMG2 sgRNA sequence (ACCATCTTATGCAGAGAACG) targeting CMG2's extracellular domain into the pSpCas9-2A-Puro vector (Addgene, #48139). Cloning of CMG2 sgRNA into pSpCas9-2A-Puro was done by following the protocol described by Feng Zhang's laboratory (54, 55). X-tremeGENE™ 9 DNA Transfection Reagent was used for transfection of the plasmids into the indicated cells following the manufacturer's manual (Roche, catalog no. 06366236001). We transfected the resulting CMG2 sgRNA construct into LLC or B16-F10 cells, resulting in the respective CMG2-KO cells, confirmed by PCR and DNA sequencing.

For cytotoxicity assays, cells grown in 96-well plates (50% confluence) were incubated with various concentrations of PA or PA variant proteins combined with 500 ng/mL LF or 100 ng/mL FP59 for 48 or 72 h. Cell viabilities were then assayed by MTT, as described previously (56), and are expressed as % of MTT signals of untreated cells. At least three biological repeats were performed. For PI/annexin V staining, ECs treated with or without toxins were collected (including the cells in medium) and resuspended in 1× binding buffer (BD Biosciences) at a concentration of 1×10^6 cells/mL. Then, 0.1 mL of the solution was stained with 5 μL each of annexin V (BD Biosciences) and 50 μg/mL PI (Invitrogen) at room temperature for 15 min. The cells were analyzed using a BD FACSCanto Flow Cytometer, and percentages of each cell population were obtained.

For assessing the effects of LF on MEK–ERK signaling, the cells were incubated with various concentrations of PA-L1-I656Q/LF for 3 h. Then, cell lysates were prepared in the modified RIPA lysis buffer containing protease inhibitors as described (56). Cell lysates were separated on SDS–PAGE gels, transferred onto nitrocellulose membranes, and analyzed by western blotting using an anti-MEK1 (#07-641, Upstate Technology), anti-MEK2 (#67410, Proteintech), anti-P-ERK (#4695, Cell Signaling), anti-c-Myc (ab32072, Abcam), or antitubulin antibody (#66031, Proteintech). Relative protein abundance was quantified using ImageJ software (https://imagej.nih.gov/ij).

Gene Expression. ECs cultured in 12-well plates were treated with or without PA-L1/LF for 4 h or 24 h; total RNA was then prepared using TRIzol reagent (Invitrogen, Carlsbad, CA). Single-strand cDNA was synthesized using reverse transcriptase reaction kit following the manufacturer's manual (Invitrogen). Expression changes of the selected key genes involved in glucose uptake, glycolysis, TCA cycle, glutaminolysis, and lipid synthesis were analyzed by real-time quantitative PCR using SYBR Green PCR Master Mix. The primer sequences are shown in *SI Appendix*, Table S1.

OCR and ECARs. Metabolic activities of tumor ECs were assessed in the XF24 Extracellular Flux analyzer (Seahorse BioScience). Tumor cells and tumor ECs grown to confluence in 24-well XF24 tissue culture plates were incubated with or without PA-L1/LF (1 μg/mL each) in pentaplicates for 24 h. Cells were changed into fresh unbuffered serum-free DMEM with 2 mM GlutaMax-1, 25 mM D-glucose, pH 7.4, and equilibrated in the medium for 1 h. Real-time ECARs and OCRs were then measured at 37°C under basal conditions and conditions following sequential additions of oligomycin (0.5 μM), FCCP (0.5 μM), and antimycin A (1 μM). ECARs and OCRs were normalized to 50 μg total protein in cell lysates. ATP production–coupled OCR is calculated as the difference between basal OCR and OCR after addition of oligomycin. Spare respiratory capacity is defined as the difference between the OCR following FCCP addition and the OCR under basal condition. Maximal respiration is defined as the difference between the OCR following FCCP addition and the OCR following oligomycin addition. Cellular ATP levels were measured using the ATPlite 1step kit (PerkinElmer).

For fatty acid oxidation assay, ECs treated with or without the toxin were changed into fresh FAO assay medium (XF base medium minimal DMEM (Seahorse BioScience, catalog no. 102353-100) with 2.5 mM D-glucose and 0.5 mM carnitine, pH 7.4) and equilibrated in the medium for 1 h. Prior to starting XF assay, the medium was replaced with FAO assay medium containing 0.20 mM palmitate–BSA or 0.20 mM BSA (Seahorse BioScience, catalog no. 102720-100).

Mice and Tumor Studies. C57BL/6J mice and C57BL/6J athymic nude (*Foxn1*$^{nu/nu}$) mice were obtained from Jackson Laboratory (Bar Harbor, Maine). *CMG2*$^{-/-}$ (whole-body) and *EC-CMG2*$^{-/-}$(endothelial cell–specific) mice were generated previously (16). Endothelial cell–specific CMG2-expressing mice (*CMG2*^{EC}) were generated as described previously with C57BL/6J background (16, 20, 21). LoxP-Stop-LoxP c-Myc transgenic mice (*c-Myc*^{LSL}) were obtained from Jackson Laboratory (#020458). To generate mice having the c-Myc transgene expressed only in ECs, the *c-Myc*^{LSL} mice were mated with *Cdh5-Cre* transgenic mice (57) (Cre recombinase under the VE-cadherin promoter) (Jackson Laboratory, #006137). For tumor studies, 10- to 14-wk-old male and female mice were used. To grow syngeneic tumors, 5×10^5 cells/mouse B16-F10 cells, 1×10^6 cells/mouse B16 (CMG2-KO) cells, or 1×10^6 cells/mouse LLC (CMG2-KO) cells were injected in the midscapular subcutis of the preshaved mice with C57BL/6J background and indicated genotypes. Visible B16-BL6 or LLC tumors (about 50 mm^3) usually formed 7 to 8 d after inoculation. To grow human C32 (BRAF^{V600E}) tumors, 5×10^6 C32 cells/mouse were injected in the midscapular subcutis of C57BL/6J athymic nude (*Foxn1*$^{nu/nu}$) mice. Tumors were treated when they became visible or at later stages and measured with digital calipers (FV Fowler Company, Inc., Newton, MA). Tumor volumes were estimated with the length, width, and height tumor dimensions using formulas: tumor volume (mm^3) = ½ (length in mm × width in mm × height in mm). Tumor-bearing mice were randomized into groups and injected intraperitoneally following schedules indicated in the figures, with PBS or the engineered toxins. Mice were weighed, and the tumors were measured before each injection. When analyzed separately by gender, no significant differences were observed between male and female mice in either tumor growth or tumor response to the toxin.

For assessing ECs in tumors using CD31 staining, B16(CMG2-KO) tumor-bearing mice treated with 2 doses of PA-L1-I656Q/LF (30 μg/15 μg) or PBS were killed by CO_2 inhalation. Tumors were harvested, fixed in 10% neutral buffered formalin for 24 h, embedded in paraffin, sectioned, and stained with a goat polyclonal anti-mouse CD31 (1:500 dilution) (sc-1506, Santa Cruz Biotechnology).

Statistics. Statistical significances of differences were calculated using unpaired or paired two-tailed Student's *t* test or one-way ANOVA when more than two groups were compared. $P < 0.05$ is considered significant difference.

Ethical Approval. All animal studies were carried out in accordance with the protocols approved by the Institutional Animal Care and Use Committee of the University of Pittsburgh (#22030855) and the National Institute of Allergy and Infectious Diseases, NIH (LPD 1E).

Data, Materials, and Software Availability. All data generated during this study are included in this article and *SI Appendix*.

ACKNOWLEDGMENTS. This research was supported by the institutional seed fund (S.L.) and the grant (R01CA254938) (S.L.) from the National Cancer Institute, NIH, and in part by Intramural Programs of the National Institute of Allergy and Infectious Diseases (S.H.L), and National Institute of Dental and Craniofacial Research (T.H.B.), NIH. We thank Mahtab Moayeri for helpful discussions and Qian Ma for help in mouse work. We thank Rasem Fattah for help in protein purification.

1. L. Bejarano, M. J. C. Jordao, J. A. Joyce, Therapeutic targeting of the tumor microenvironment. *Cancer Discov.* **11**, 933–959 (2021).
2. R. Baghban *et al.*, Tumor microenvironment complexity and therapeutic implications at a glance. *Cell Commun. Signal* **18**, 59 (2020).
3. H. Hurwitz, Integrating the anti-VEGF-A humanized monoclonal antibody bevacizumab with chemotherapy in advanced colorectal cancer. *Clin. Colorectal. Cancer* **4**, S62–68 (2004).
4. H. Hurwitz *et al.*, Bevacizumab plus irinotecan, fluorouracil, and leucovorin for metastatic colorectal cancer. *N. Engl. J. Med.* **350**, 2335–2342 (2004).
5. M. Schmittnaegel *et al.*, Dual angiopoietin-2 and VEGFA inhibition elicits antitumor immunity that is enhanced by PD-1 checkpoint blockade. *Sci. Transl. Med.* **9**, eaak9670 (2017).
6. G. Bergers, D. Hanahan, Modes of resistance to anti-angiogenic therapy. *Nat. Rev. Cancer* **8**, 592–603 (2008).
7. D. F. Quail *et al.*, The tumor microenvironment underlies acquired resistance to CSF-1R inhibition in gliomas. *Science* **352**, aad3018 (2016).
8. J. Cui, F. Shao, Biochemistry and cell signaling taught by bacterial effectors. *Trends Biochem. Sci.* **36**, 532–540 (2011).
9. I. Antic, M. Biancucci, Y. Zhu, D. R. Gius, K. J. Satchell, Site-specific processing of Ras and Rap1 Switch I by a MARTX toxin effector domain. *Nat. Commun.* **6**, 7396 (2015).
10. B. Schorch *et al.*, Targeting oncogenic Ras by the Clostridium perfringens toxin TpeL. *Oncotarget* **9**, 16489–16500 (2018).
11. S. Liu, M. Moayeri, S. H. Leppla, Anthrax lethal and edema toxins in anthrax pathogenesis. *Trends Microbiol.* **22**, 317–325 (2014).
12. S. Liu *et al.*, Solid tumor therapy by selectively targeting stromal endothelial cells. *Proc. Natl. Acad. Sci. U. S. A.* **113**, E4079–4087 (2016).
13. S. Liu *et al.*, Intermolecular complementation achieves high-specificity tumor targeting by anthrax toxin. *Nat. Biotechnol.* **23**, 725–730 (2005).
14. C. Bachran, S. H. Leppla, Tumor targeting and drug delivery by anthrax toxin. *Toxins (Basel)* **8** (2016).
15. M. Moayeri, S. H. Leppla, C. Vrentas, A. P. Pomerantsev, S. Liu, Anthrax pathogenesis. *Annu. Rev. Microbiol.* **69**, 185–208 (2015).
16. S. Liu *et al.*, Capillary morphogenesis protein-2 is the major receptor mediating lethality of anthrax toxin in vivo. *Proc. Natl. Acad. Sci. U. S. A.* **106**, 12424–12429 (2009).
17. C. Merritt *et al.*, Imaging of anthrax intoxication in mice reveals shared and individual functions of surface receptors CMG-2 and TEM-8 in cellular toxin entry. *J. Biol. Chem.* **298**, 101467 (2021).
18. K. H. Chen, S. Liu, L. A. Bankston, R. C. Liddington, S. H. Leppla, Selection of anthrax toxin protective antigen variants that discriminate between the cellular receptors TEM8 and CMG2 and achieve targeting of tumor cells. *J. Biol. Chem.* **282**, 9834–9846 (2007).

19. Z. Zuo *et al.*, A potent tumor-selective ERK pathway inactivator with high therapeutic index. *PNAS Nexus* **1**, pgac104 (2022).
20. S. Liu *et al.*, Anthrax toxin targeting of myeloid cells through the CMG2 receptor Is essential for establishment of *Bacillus anthracis* infections in mice. *Cell Host. Microbe.* **8**, 455–462 (2010).
21. S. Liu *et al.*, Key tissue targets responsible for anthrax-toxin-induced lethality. *Nature* **501**, 63–68 (2013).
22. S. M. Weis, D. A. Cheresh, Tumor angiogenesis: Molecular pathways and therapeutic targets. *Nat. Med.* **17**, 1359–1370 (2011).
23. R. Noy, J. W. Pollard, Tumor-associated macrophages: From mechanisms to therapy. *Immunity* **41**, 49–61 (2014).
24. P. GascardT. D. Isty, Carcinoma-associated fibroblasts: Orchestrating the composition of malignancy. *Genes. Dev.* **30**, 1002–1019 (2016).
25. K. Shiga *et al.*, Cancer-associated fibroblasts: Their characteristics and their roles in tumor growth. *Cancers (Basel)* **7**, 2443–2458 (2015).
26. G. J. Yuen, E. Demissie, S. Pillai, B lymphocytes and cancer: A love-hate relationship. *Trends Cancer* **2**, 747–757 (2016).
27. C. Liu, C. J. Workman, D. A. Vignali, Targeting regulatory T cells in tumors. *FEBS J.* **283**, 2731–2748 (2016).
28. B. Chaudhary, E. Elkord, Regulatory T cells in the tumor microenvironment and cancer progression: Role and therapeutic targeting. *Vaccines (Basel)* **4**, 28 (2016).
29. K. H. Chen *et al.*, Anthrax toxin protective antigen variants that selectively utilize either the CMG2 or TEM8 receptors for cellular uptake and tumor targeting. *J. Biol. Chem.* **291**, 22021–22029 (2016).
30. S. Liu, Q. Ma, R. Fattah, T. H. Bugge, S. H. Leppla, Anti-tumor activity of anthrax toxin variants that form a functional translocation pore by intermolecular complementation. *Oncotarget* **8**, 65123–65131 (2017).
31. D. D. Phillips *et al.*, Engineering anthrax toxin variants that exclusively form octamers and their application to targeting tumors. *J. Biol. Chem.* **288**, 9058–9065 (2013).
32. A. N. Wein *et al.*, An anthrax toxin variant with an improved activity in tumor targeting. *Sci. Rep.* **5**, 16267 (2015).
33. S. Liu, H. Aaronson, D. J. Mitola, S. H. Leppla, T. H. Bugge, Potent antitumor activity of a urokinase-activated engineered anthrax toxin. *Proc. Natl. Acad. Sci. U. S. A.* **100**, 657–662 (2003).
34. S. Liu, S. Netzel-Arnett, H. Birkedal-Hansen, S. H. Leppla, Tumor cell-selective cytotoxicity of matrix metalloproteinase-activated anthrax toxin. *Cancer Res.* **60**, 6061–6067 (2000).
35. S. Liu *et al.*, Matrix metalloproteinase-activated anthrax lethal toxin demonstrates high potency in targeting tumor vasculature. *J. Biol. Chem.* **283**, 529–540 (2008).
36. N. Arora, K. R. Klimpel, Y. Singh, S. H. Leppla, Fusions of anthrax toxin lethal factor to the ADP-ribosylation domain of *Pseudomonas* exotoxin A are potent cytotoxins which are translocated to the cytosol of mammalian cells. *J. Biol. Chem.* **267**, 15542–15548 (1992).
37. P. S. Ward, C. B. Thompson, Metabolic reprogramming: A cancer hallmark even warburg did not anticipate. *Cancer Cell* **21**, 297–308 (2012).
38. G. Kroemer, J. Pouyssegur, Tumor cell metabolism: Cancer's Achilles' heel. *Cancer Cell* **13**, 472–482 (2008).
39. Z. E. Stine, Z. E. Walton, B. J. Altman, A. L. Hsieh, C. V. Dang, MYC, metabolism, and Cancer. *Cancer Discov.* **5**, 1024–1039 (2015).
40. A. L. Hsieh, Z. E. Walton, B. J. Altman, Z. E. Stine, C. V. Dang, MYC and metabolism on the path to cancer. *Semin. Cell Dev. Biol.* **43**, 11–21 (2015).
41. R. Lugano, M. Ramachandran, A. Dimberg, Tumor angiogenesis: Causes, consequences, challenges and opportunities. *Cell Mol. Life Sci.* **77**, 1745–1770 (2020).
42. Z. Nie *et al.*, c-Myc is a universal amplifier of expressed genes in lymphocytes and embryonic stem cells. *Cell* **151**, 68–79 (2012).
43. C. V. Dang, MYC on the path to cancer. *Cell* **149**, 22–35 (2012).
44. M. Welcker *et al.*, The Fbw7 tumor suppressor regulates glycogen synthase kinase 3 phosphorylation-dependent c-Myc protein degradation. *Proc. Natl. Acad. Sci. U.S.A.* **101**, 9085–9090 (2004).
45. M. Yada *et al.*, Phosphorylation-dependent degradation of c-Myc is mediated by the F-box protein Fbw7. *EMBO J.* **23**, 2116–2125 (2004).
46. N. Ricard, S. Bailly, C. Guignabert, M. Simons, The quiescent endothelium: Signalling pathways regulating organ-specific endothelial normalcy. *Nat. Rev. Cardiol.* **18**, 565–580 (2021).
47. S. Liu *et al.*, Diphthamide modification on eukaryotic elongation factor 2 is needed to assure fidelity of mRNA translation and mouse development. *Proc. Natl. Acad. Sci. U. S. A.* **109**, 13817–13822 (2012).
48. J. C. Milne, D. Furlong, P. C. Hanna, J. S. Wall, R. J. Collier, Anthrax protective antigen forms oligomers during intoxication of mammalian cells. *J. Biol. Chem.* **269**, 20607–20612 (1994).
49. N. Arora, S. H. Leppla, Fusions of anthrax toxin lethal factor with shiga toxin and diphtheria toxin enzymatic domains are toxic to mammalian cells. *Infect. Immun.* **62**, 4955–4961 (1994).
50. P. K. Gupta, M. Moayeri, D. Crown, R. J. Fattah, S. H. Leppla, Role of N-terminal amino acids in the potency of anthrax lethal factor. *PLoS One* **3**, e3130 (2008).
51. A. P. Pomerantsev *et al.*, A *Bacillus anthracis* strain deleted for six proteases serves as an effective host for production of recombinant proteins. *Protein Expr. Purif.* **80**, 80–90 (2011).
52. M. S. O'Reilly *et al.*, Angiostatin: A novel angiogenesis inhibitor that mediates the suppression of metastases by a Lewis lung carcinoma. *Cell* **79**, 315–328 (1994).
53. L. E. Reynolds, K. M. Hodivala-Dilke, Primary mouse endothelial cell culture for assays of angiogenesis. *Methods Mol. Med.* **120**, 503–509 (2006).
54. N. E. Sanjana, O. Shalem, F. Zhang, Improved vectors and genome-wide libraries for CRISPR screening. *Nat. Methods* **11**, 783–784 (2014).
55. J. Liu, Z. Zuo, M. Zou, T. Finkel, S. Liu, Identification of the transcription factor Miz1 as an essential regulator of diphthamide biosynthesis using a CRISPR-mediated genome-wide screen. *PLoS Genet.* **16**, e1009068 (2020).
56. S. Liu, S. H. Leppla, Cell surface tumor endothelium marker 8 cytoplasmic tail-independent anthrax toxin binding, proteolytic processing, oligomer formation, and internalization. *J. Biol. Chem.* **278**, 5227–5234 (2003).
57. J. A. Alva *et al.*, VE-Cadherin-Cre-recombinase transgenic mouse: A tool for lineage analysis and gene deletion in endothelial cells. *Dev. Dyn.* **235**, 759–767 (2006).